DOI: 10.1002/adma.200792876

Self-Organized Buffer Layers in Organic Solar Cells**

By *Qingshuo Wei, Takeshi Nishizawa, Keisuke Tajima,** and *Kazuhito Hashimoto**

The self-organization of organic molecules is an attractive approach for nanostructure fabrication.[1–4] The control of layered structures on the nanoscale is particularly desirable in thin-film organic devices because this largely affects the electrical, optical, and mechanical properties of the films. To spontaneously fabricate such multilayered structures, the careful control of driving forces such as phase separation, crystallization, or the surface energy of the materials is necessary. For example, Goffri et al. reported the spontaneous formation of bilayer structures between poly(3-hexylthiophene) (P3HT) and polyethylene in mixture films.[5] The crystallization of polyethylene induces the effective encapsulation of P3HT at the organic-semiconductor/dielectric interface, resulting in mechanically robust and high-performance thin-film transistors. Very recently, Krishnan et al. reported a new method of obtaining self-organized multilayer structures at the nanoscale level.[6] The spin-coated films from the mixtures of the nanoparticles and the polymers were simply annealed to achieve the accumulation of the nanoparticles to the substrate surface owing to the entropic and enthalpic driving forces. These pioneering studies proposed new attractive approaches for the fabrication of various organic thin-film devices. However, studies of the self-organized bilayer or multilayer structure of functional materials are still very limited and remain challenging. Moreover, their applications to actual electronic devices have been hardly explored.

In the present work, we report a novel, simple approach to form layered structures in organic thin films by controlling the surface energy of the materials and its application to organic solar cells. It is well-known that materials having a low surface energy such as fluorinated or silicone compounds prefer to migrate to the air/liquid interface during coating.[7–10] This is called surface segregation, which is driven by the total energy minimization of the system. On the basis of the idea to utilize this phenomenon, we designed and synthesized a novel fullerene derivative with a fluorocarbon chain (F-PCBM), as shown in Figure 1a. The C_{60} part works as an electron-accepting and -transporting material and the perfluoroalkyl group gives a low surface energy to the material. When a small amount of F-PCBM is mixed in the solution for spin-coating, it is expected that the F-PCBM spontaneously migrates to the surface of the organic layer during spin-casting owing to the low surface energy of the fluorocarbon, and forms a very thin layer of F-PCBM in a single step (Fig. 1b). After the deposition of the metal electrode, it could act as a buffer layer between the polymer and the metal electrode, which may decrease the hole–electron recombination loss and leaking current at the P3HT/Al interface.[11–14] Furthermore, the perfluoroalkyl chains could form an interfacial dipole moment with its negative pole pointing towards the aluminum. It could shift the vacuum level in the solid state (i.e., it decreases the metal work function or increases the highest occupied and lowest unoccupied molecular orbital (HOMO and LUMO) levels of the organic layer). As a result, the energy barrier for electron injection and collection could be reduced, as shown schematically in Figure 1c and d.[15–19]

F-PCBM was prepared by following the synthesis procedure in Scheme 1. Starting from [6,6]-phenyl-C_{61}-butyric acid methyl ester (PCBM), the carboxylic acid derivative was obtained by treatment with HCl and acetic acid in toluene. It was further reacted with thionyl chloride in CS_2 solution to form the corresponding carbonyl chloride. F-PCBM was synthesized by reacting the carbonyl chloride with 1*H*, 1*H*-pentadecafluoro-1-octanol in the presence of sodium hydride. The product was purified by silica column chromatography and obtained as dark brown powder with high purity. The product was characterized from ^{1}H NMR, ^{19}F NMR, and ^{13}C NMR spectra and by high-resolution matrix-assisted laser desorption ionization time-of-flight mass spectrometry (MALDI-TOF-MS). The F-PCBM was thermally and air stable, and soluble in common solvents such as chloroform, chlorobenzene, and toluene.

The cyclic voltammograms of both the PCBM and the F-PCBM in dichloromethane are shown in Figure 2a. Both voltammograms exhibit three well-defined, single-electron, quasireversible waves in this scanning range. The reduction waves of the F-PCBM were observed at almost the same potentials as that of PCBM. The half-cell potentials for the reduction of the F-PCBM and PCBM relative to Ag/Ag^+ were −580 mV, −960 mV, −1462 mV, and −596 mV, −984 mV, −1479 mV, respectively. This result suggests that the LUMO levels and electron-accepting ability of F-PCBM were not significantly

[*] Dr. K. Tajima, Prof. K. Hashimoto, Q. Wei, T. Nishizawa
Department of Applied Chemistry, School of Engineering
The University of Tokyo
7-3-1 Hongo, Bunkyo-ku, Tokyo 113-8656 (Japan)
E-mail: k-tajima@light.t.u-tokyo.ac.jp;
hashimoto@light.t.u-tokyo.ac.jp
Prof. K. Hashimoto
HASHIMOTO Light Energy Conversion Project
Exploratory Research for Advanced Technology (ERATO)
Japan Science Technology Agency (JST)
Hongo, Bunkyo-ku, Tokyo 113-8656 (Japan)

[**] We thank Prof. Seki (Nagoya University) and Dr. Yoshida (The University of Tokyo) for helpful discussions, Dr. Mori and Mr. Miyazaki (Sumitomo Heavy Industries) for photoelectron yield spectroscopy measurements, Dr. Nakano for ^{19}F NMR measurements, and Mr. Miyanishi for the polymer synthesis. Supporting Information is available online from Wiley InterScience or from the authors.

ADVANCED MATERIALS

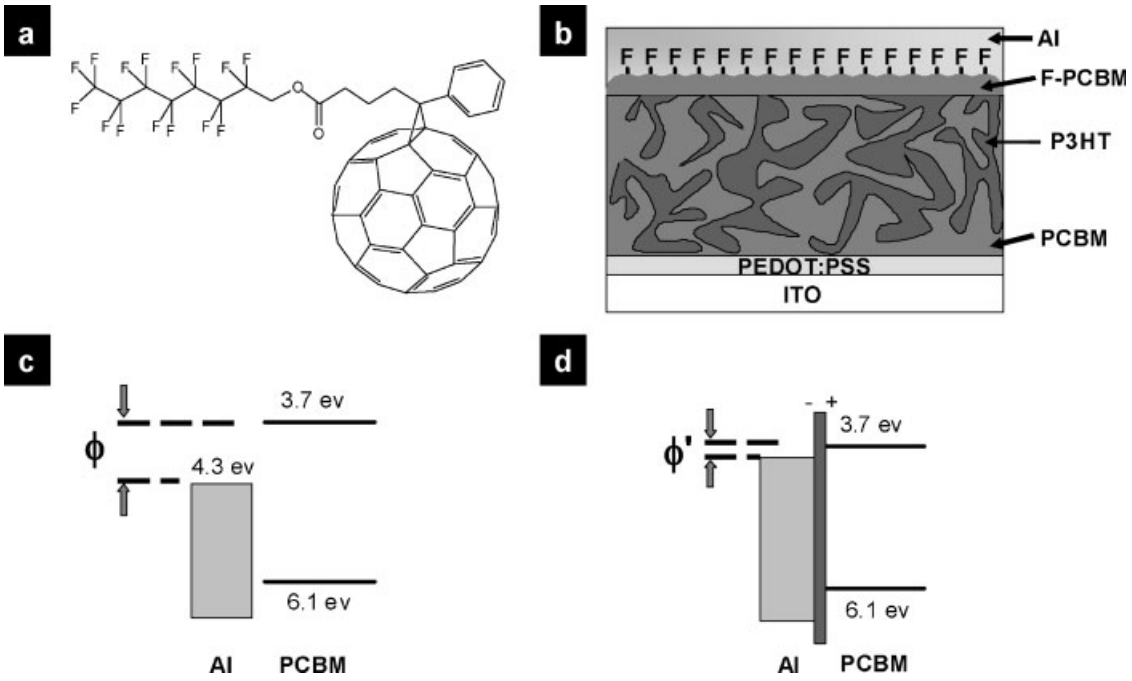

Figure 1. a) Chemical structure of F-PCBM. b) Schematic representation of bulk heterojunction solar cells with a buffer layer of the fluoride compound; schematic energy diagrams of the interface between [6,6]-phenyl-C_{61}-butyric acid methyl ester (PCBM) and top electrode Al c) without and d) with a dipole moment layer between them. ϕ and ϕ' are the electron injection barriers before and after the introduction of F-PCBM, respectively.

affected by introducing the fluorocarbon chain on PCBM. The UV-vis absorption spectra of F-PCBM and PCBM were measured in chloroform solution at room temperature (Fig. 2b). Both spectra showed the same absorption pattern with maximums at 260 nm and 329 nm, indicating that the F-PCBM has the same optical band gap as the PCBM. From the results shown above, we conclude that the introduction of the fluorocarbon does not affect the energy level of the C_{60} group.

To investigate the surface segregation of F-PCBM during spin coating, depth profiling of X-ray photoelectron spectroscopy (XPS) was carried out. Film samples of P3HT:PCBM: F-PCBM (1:0.8:0.1, w/w) and PCBM:F-PCBM (0.8:0.1, w/w)

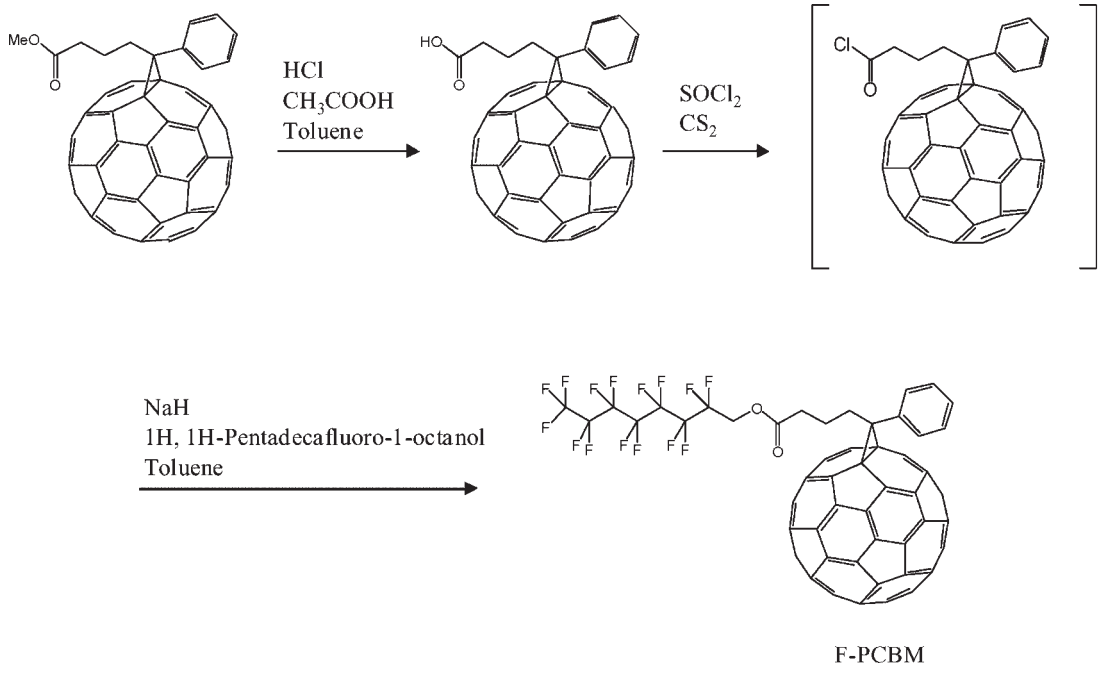

Scheme 1. Synthesis route of F-PCBM.

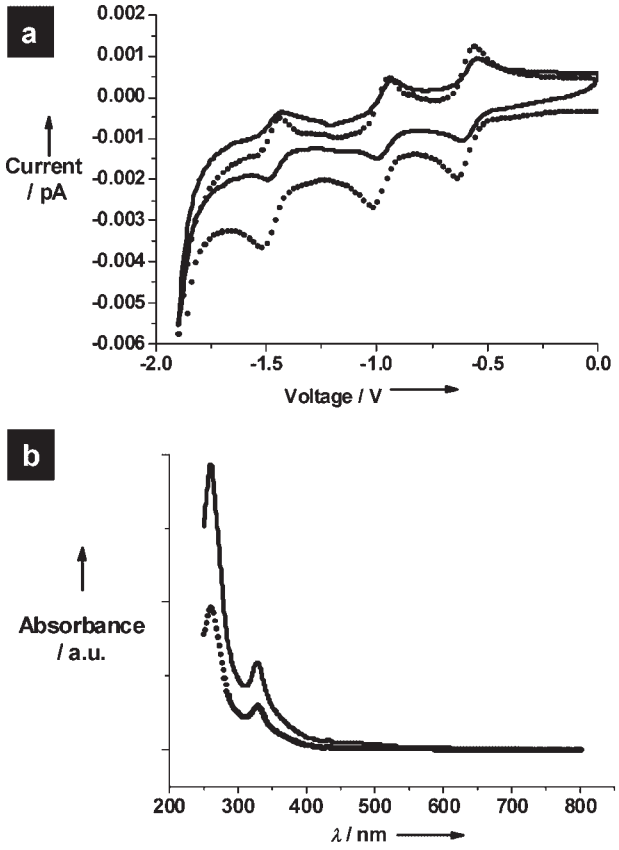

Figure 2. a) Cyclic voltammograms in dichloromethane and b) UV-vis spectra in chloroform of PCBM (dotted line) and F-PCBM (full line).

blends were prepared on quartz substrates. The film thicknesses were determined as 103 nm and 38 nm, respectively, using the interference fringe of X-ray diffraction analysis at a low angle. Sample etching was performed using Ar^+ ions with a 500 V accelerated voltage. The raster area was approximately 1×1 cm^2, and the etching rate range was estimated as 0.3–0.4 nm s^{-1}. After each sputtering cycle, XPS spectra were obtained by Mg Kα radiation. Figure 3 shows the region of the F 1s in the XPS spectra for both the P3HT:PCBM:F-PCBM and PCBM:F-PCBM films after the corresponding sputtering time. For the samples without etching, the peak of F 1s can be clearly observed at 690 eV. After 5 s sputtering (corresponding to about 2 nm of layer thickness), the F 1s peaks completely disappeared in both cases. Etching was carried out until the entire organic layer was removed, and no fluoride peaks were detected other than at the surface. Therefore, it is concluded that F-PCBM exists only within the range of 2 nm at the top, which is comparable to the thickness of the F-PCBM monolayer. The results of XPS depth profiling strongly support our hypothesis that F-PCBM is apt to migrate to the surface of the active layer owing to the low surface energy.

The F-PCBM layer spontaneously formed by spin-coating was used in organic solar cells as the buffer layer. For the device fabrication, an active layer of P3HT:PCBM = 1:0.8 (w/w) was spin coated on indium tin oxide (ITO)-coated glass/poly(3,4-ethylenedioxythiophene):poly(styrene sulfonic acid) (PEDOT:PSS) substrates and an Al electrode was subsequently evaporated on the top of the active layer. The thickness of the active layer was ca. 100 nm and the device area was 0.03 cm^2, which was defined by a photo mask. Annealing was performed at 150 °C for 5 min under N_2 atmosphere after the deposition of the Al electrode. The ratios between P3HT and PCBM and the active layer thickness were optimized to achieve the highest efficiency. Figure 4 shows typical current–voltage (*I–V*) curves for devices with and without F-PCBM in the solution under 100 mW cm^{-2} simulated solar light irradiation (AM 1.5). The conventional P3HT:PCBM bulk heterojunction device (without F-PCBM) showed a short-circuit current density (I_{SC}) of 8.72 mA cm^{-2}, an open-circuit voltage (V_{OC}) of 0.55 V, and a fill factor (*FF*) of 0.64, resulting in a power conversion efficiency (PCE) of 3.09%. When a small amount of F-PCBM was mixed in the spin-coated solution (P3HT:PCBM:F-PCBM = 1:0.8:0.1 w/w), a considerable improvement of the PCE up to 3.79% was observed with values for I_{SC} of 9.51 mA cm^{-2}, V_{OC} of 0.57 V, and *FF* of 0.70. Note that the *FF* shows quite a high

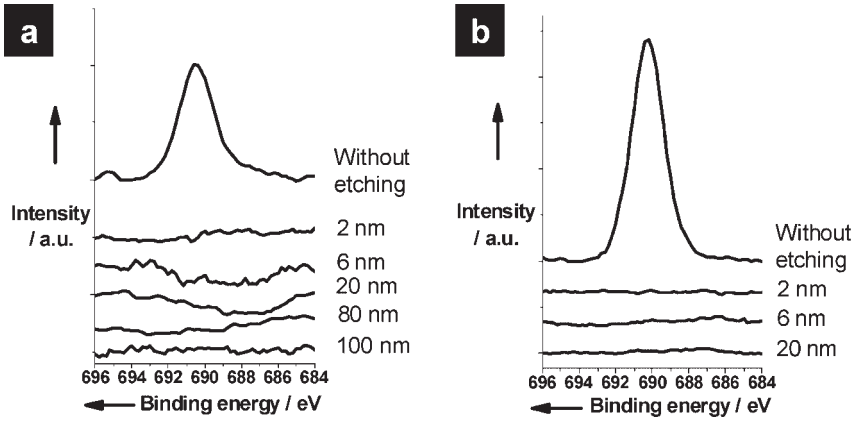

Figure 3. XPS F 1s spectra of a) as-cast P3HT:PCBM:F-PCBM films without etching, after etching for 2 nm, 6 nm, 20 nm, 80 nm and 100 nm and of b) as-cast PCBM: F-PCBM films without etching, after etching for 2 nm, 6 nm and 20 nm. The film thicknesses were 103 nm and 38 nm for (a) and (b), respectively.

ADVANCED MATERIALS

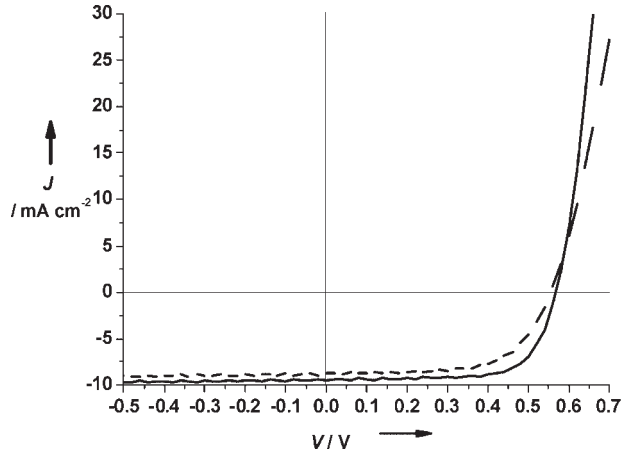

Figure 4. *I–V* characteristics under 100 mW cm^2 AM1.5 illumination of P3HT:PCBM bulk heterojunction devices with F-PCBM (full line) and without F-PCBM (dotted line).

value, and the best value we achieved was 0.72. This is, to the best of our knowledge, the highest *FF* reported in organic solar cells. The series resistances of the devices were also calculated from the slope of the *I–V* curve close to 1 V in the dark. As a result, a significant decrease in series resistance was observed in the device with F-PCBM (Table 1).

The device results indicate that the F-PCBM buffer layer improves device performance, particularly the fill factor and short-circuit current. To clarify the reason for this, we investigated the role of F-PCBM. The surface morphologies of both P3HT:PCBM:F-PCBM and P3HT:PCBM films were observed by atomic force microscopy (AFM). The AFM height images showed no significant difference in the films with and without F-PCBM (Fig. S5). UV-vis and XPS depth-profiling measurements were also conducted and revealed that neither the film thickness nor the composition inside the active layer was affected by the introduction of F-PCBM. Therefore, we attributed the improvement in the device performance to the modified interface between the active layer and the Al electrode. One possibility is the energy level matching of PCBM and the Al electrode induced by the dipole moment layer of F-PCBM (Fig. 1c and d). In other words, the electron injection barrier between PCBM and Al was lowered by introducing F-PCBM, which reduced series resistance of the devices resulting in the improved fill factor and the short-circuit current.[20] A similar mechanism has been proposed for the other buffer layers such as LiF in the case of organic light-emitting diodes, which is successively deposited on organic layers in vacuum.[21,22]

Table 1. Summary of performance of devices with and without F-PCBM.

	PCE [%]	I_{SC} [mA cm^{-2}]	*FF*	V_{OC} [V]	R_{SA} [Ω cm^2]
With F-PCBM [a]	3.79	9.51	70.0	0.57	2.88
Without F-PCBM [b]	3.09	8.72	64.4	0.55	4.54

[a]P3HT:PCBM:F-PCBM = 1:0.8:0.1 (w/w). [b]P3HT:PCBM = 1:0.8 (w/w).

To investigate the interfacial dipole moment in the devices, ionization potential (*IP*) measurements were carried out on the spin-coated films by photoelectron yield spectroscopy (PYS). To simplify the issue, we first measured the *IP* of the pristine PCBM film with and without the addition of F-PCBM. As shown in Figure 5a, the *IP* of PCBM was 6.0 eV, which was close to the value previously reported (6.1 eV).[23] When a small amount of F-PCBM was added in the solution for the film preparation, *IP* shifted to 6.33 eV. By considering the same energy levels between F-PCBM and PCBM, the increase in *IP* should be attributed to the aligned surface dipole moment. The *IP* shift induced by a uniform dipolar surface layer can be estimated from classical electrostatics.[24] If the presence of the F-PCBM monolayer was assumed (F-PCBM forms a monolayer or sub-monolayer at the top according to the XPS depth profiling measurement) and the fluorocarbon chain was vertically standing on the surface, the expected *IP* shift was calculated to be 0.36 eV, which corresponds to our experimental results (0.33 eV).[18,24,25] The calculation method is shown in the Supporting Information. Although some approximations

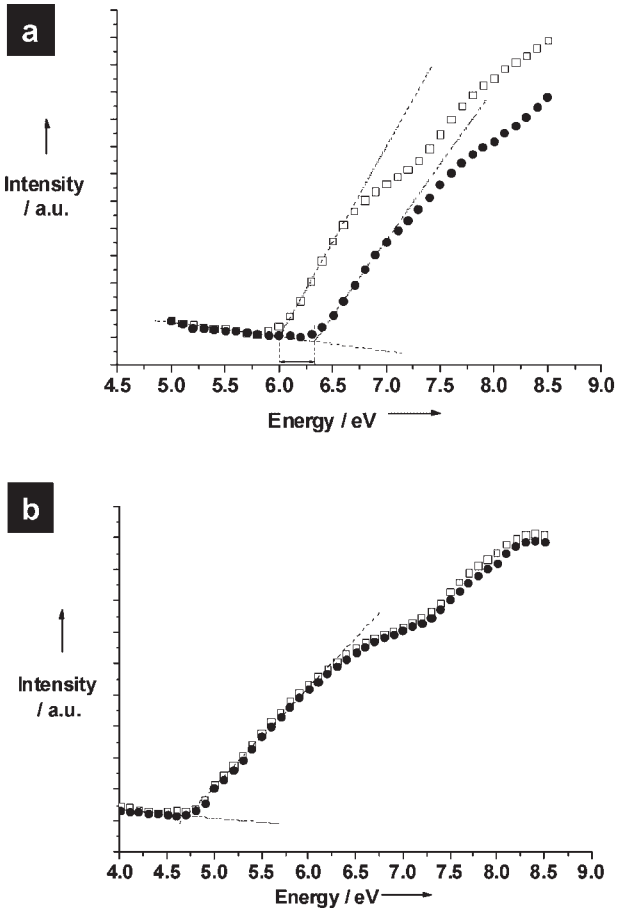

Figure 5. Photoelectron yield spectroscopy for a) PCBM (open squares) and PCBM:F-PCBM films (closed circles), and for b) P3HT:PCBM-blended (open squares) and P3HT:PCBM:F-PCBM films (closed circles).

are involved in the calculation, we believe that the fluorocarbon chain could be packed on the surface with good alignment, causing a significant shift in *IP*. This hypothesis is also supported by previous studies of the surface orientation of perfluoroalkyl groups in copolymer films.[26] Figure 5b shows the PYS results of the P3HT:PCBM-blended films with and without F-PCBM. The *IP* of P3HT is approximately 4.7 eV, which is close to the reported values (4.65–5.1 eV).[27–30] In contrast to the PCBM films, no significant difference in the *IP* of P3HT was observed by the introduction of F-PCBM. The absence of a shift in the *IP* of P3HT disagrees with the assumption of the uniform dipole layer formation on the P3HT: PCBM layer. One possibility is that the F-PCBM layer is laterally inhomogeneous on the surface of the P3HT: PCBM blended film.[31] If the domains of PCBM and P3HT are exposed on the surface, F-PCBM might accumulate on the surface of the PCBM domain and form a dipole moment layer similar to that in the case of a pure PCBM film. On the P3HT domains, however, the layer of F-PCBM might be less dense and the fluoroalkyl chains might be less oriented because of the small interaction between the C_{60} group and the surface. Note that electron collection occurs mainly from the LUMO of PCBM, not from P3HT, to the Al electrode in the devices. Therefore, we believe that the surface dipole moment induced by the F-PCBM layer could be the origin of the improvement in the device performance, although other explanations are still possible. Further investigation of these blended films using electrostatic force and surface potential microscopy is underway.

In conclusion, a novel fullerene derivative with fluorocarbon chain (F-PCBM) was synthesized and successfully applied in bulk-heterojunction polymer solar cells. The addition of a small amount of F-PCBM to the solution improved the photovoltaic performance, particularly *FF*, because of the spontaneous formation of the thin buffer layer of F-PCBM. The generality of the current approach and compatibility to the solution processes have a large advantage for application to various organic electronic devices. It is also expected that the current approach can be applicable to other solution-based coating processes.

Experimental

All electrochemical measurements were performed using a HSV-100 (Hokuto Denko) electrochemical workstation. The experimental setup contained a carbon working electrode (PFCE-1, purchased from BAS, Japan), a Pt wire counter electrode, and a silver wire reference electrode. Anhydrous dichloromethane was used as an electrolyte, containing 0.1 m tetrabutylammonium perchlorate and approximately 1 mm F-PCBM or PCBM.

Absorption spectra were measured using a SHIMADZU spectrophotometer MPC-3100. AFM measurement was carried out using a Digital Instrumental Nanoscope 31 operated in tapping mode.

Depth profiling experiments were performed using a JPS-9010MC XPS spectrometer. Mg Kα radiation was used in the measurement. Sample etching was performed using an argon ion etcher with a 500 V accelerated voltage. The etch area was approximately 1×1 cm^2. The etching rate was approximately within 0.3–0.4 nm s^{-1}, which is calculated from the time for removing the entire organic layer.

Solar cells were prepared with the structure of ITO/PEDOT:PSS/active layer/Al. ITO-coated glass substrates were cleaned by ultrasonication in detergent, water, acetone, and 2-propanol. After drying the substrate at 90 °C for 20 min, PEDOT:PSS (Baytron P) was spin-coated (3000 rpm for 30 s) on ITO. The film was dried at 140 °C in the air for 30 min. After cooling down the substrate, chlorobenzene solution of the P3HT, PCBM, and F-PCBM mixture was spin-coated. The concentration of P3HT was 10 mg mL^{-1}. Al electrodes were then evaporated under high vacuum (lower than 1×10^{-3} Pa) in the ULVAC UPC-260F vacuum evaporation system. The thickness of the Al electrode was approximately 100 nm. Post-device annealing was carried out at 150 °C for 5 min inside a nitrogen-filled glove-box. The active area of the device irradiated by the light was defined by a photo mask as 1×3 mm^2.

The current–voltage characteristics of the solar cells were measured using the Agilent Technologies E5273A C-V measurement system. PCE was examined using a xenon-lamp-based solar simulator (Peccell Technologies PCE-L11). Light intensity was adjusted by a standard silicon solar cell (Bunkou Keiki BS520).

Photoelectron yield spectroscopy was performed using the ionization potential measurement system PYS-201 (Sumitomo Heavy Industries Advanced Machinery Co., Ltd.).

Received: November 20, 2007
Published online:

[1] J.-M. Lehn, *Angew. Chem. Int. Ed. Engl.* **1990**, *29*, 1304.
[2] G. M. Whitesides, J. P. Mathias, C. T. Seto, *Science* **1991**, *254*, 1312.
[3] F. J. M. Hoeben, P. Jonkheijm, E. W. Meijer, A. Schenning, *Chem. Rev.* **2005**, *105*, 1491.
[4] T. Nishizawa, K. Tajima, K. Hashimoto, *J. Mater. Chem.* **2007**, *17*, 2440.
[5] S. Goffri, C. Muller, N. Stingelin-Stutzmann, D. W. Breiby, C. P. Radano, J. W. Andreasen, R. Thompson, R. A. J. Janssen, M. M. Nielsen, P. Smith, H. Sirringhaus, *Nat. Mater.* **2006**, *5*, 950.
[6] R. S. Krishnan, M. E. Mackay, P. M. Duxbury, A. Pastor, C. J. Hawker, B. Van Horn, S. Asokan, M. S. Wong, *Nano Lett.* **2007**, *7*, 484.
[7] D. R. Iyengar, S. M. Perutz, C. A. Dai, C. K. Ober, E. J. Kramer, *Macromolecules* **1996**, *29*, 1229.
[8] S. Affrossman, P. Bertrand, M. Hartshorne, T. Kiff, D. Leonard, R. A. Pethrick, R. W. Richards, *Macromolecules* **1996**, *29*, 5432.
[9] R. Benrashid, G. L. Nelson, J. H. Linn, K. H. Hanley, W. R. Wade, *J. Appl. Polym. Sci.* **1993**, *49*, 523.
[10] X. Chen, J. A. Gardella, *Macromolecules* **1994**, *27*, 3363.
[11] C. J. Brabec, S. E. Shaheen, C. Winder, N. S. Sariciftci, P. Denk, *Appl. Phys. Lett.* **2002**, *80*, 1288.
[12] V. Shrotriya, G. Li, Y. Yao, C. W. Chu, Y. Yang, *Appl. Phys. Lett.* **2006**, *88*, 073508.
[13] G. Li, C. W. Chu, V. Shrotriya, J. Huang, Y. Yang, *Appl. Phys. Lett.* **2006**, *88*, 253503.
[14] F. L. Zhang, M. Ceder, O. Ingands, *Adv. Mater.* **2007**, *19*, 1835.
[15] H. Ishii, K. Sugiyama, E. Ito, K. Seki, *Adv. Mater.* **1999**, *11*, 605.
[16] X. Crispin, *Sol. Energy Mater. Sol. Cells* **2004**, *83*, 147.
[17] S. Khodabakhsh, B. M. Sanderson, J. Nelson, T. S. Jones, *Adv. Funct. Mater.* **2006**, *16*, 95.
[18] B. de Boer, A. Hadipour, M. M. Mandoc, T. van Woudenbergh, P. W. M. Blom, *Adv. Mater.* **2005**, *17*, 621.
[19] J. Kim, J. Park, J. Lee, J. Jang, D. Kim, K. Cho, *Appl. Phys. Lett.* **2007**, *91*, 112111.
[20] C. Brabec, in *Organic Photovoltaics: Concepts and Realization*, (Eds: C. Brabec, V. Dyakonov, J. Parisi, N. S. Sariciftci), Springer, Heidelberg, Germany **2003**, pp. 159–248.

ADVANCED MATERIALS

[21] L. S. Hung, C. W. Tang, M. G. Mason, *Appl. Phys. Lett.* **1997**, *70*, 152.
[22] G. E. Jabbour, B. Kippelen, N. R. Armstrong, N. Peyghambarian, *Appl. Phys. Lett.* **1998**, *73*, 1185.
[23] C. Winder, D. Muhlbacher, H. Neugebauer, N. S. Sariciftci, C. Brabec, R. A. J. Janssen, J. K. Hummelen, *Mol. Cryst. Liq. Cryst.* **2002**, *385*, 213.
[24] R. W. Zehner, B. F. Parsons, R. P. Hsung, L. R. Sita, *Langmuir* **1999**, *15*, 1121.
[25] D. M. Alloway, M. Hofmann, D. L. Smith, N. E. Gruhn, A. L. Graham, R. Colorado, V. H. Wysocki, T. R. Lee, P. A. Lee, N. R. Armstrong, *J. Phys. Chem. B* **2003**, *107*, 11690.
[26] J. Genzer, E. Sivaniah, E. J. Kramer, J. G. Wang, H. Korner, M. L. Xiang, K. Char, C. K. Ober, B. M. DeKoven, R. A. Bubeck, M. K. Chaudhury, S. Sambasivan, D. A. Fischer, *Macromolecules* **2000**, *33*, 1882.
[27] Y. Sohn, J. T. Stuckless, *Chem. Phys. Lett.* **2007**, *436*, 228.
[28] D. Chirvase, Z. Chiguvare, A. Knipper, J. Parisi, V. Dyakonov, J. C. Hummelen, *Synth. Met.* **2003**, *138*, 299.
[29] A. J. Cascio, J. E. Lyon, M. M. Beerbom, R. Schlaf, Y. Zhu, S. A. Jenekhe, *Appl. Phys. Lett.* **2006**, *88*, 062104.
[30] M. Onoda, K. Tada, H. Nakayama, *J. Appl. Phys.* **1999**, *86*, 2110.
[31] R. Schlaf, A. Klein, C. Pettenkofer, W. Jaegermann, *Phys. Rev. B* **1993**, *48*, 14242.